

Study of the ω/ω_3 , ρ/ρ_3 and the newly observed ω -like state $X(2220)$

Ya-Rong Wang^{1,2} ^{*} Ting-Yan Li^{1,2} [†] Zheng-Yuan Fang^{1,2} [‡] Hao Chen^{1,2,3} [§] and Cheng-Qun Pang^{1,4} ^{¶**}

¹College of Physics and Electronic Information Engineering, Qinghai Normal University, Xining 810000, China

²Joint Research Center for Physics, Lanzhou University and Qinghai Normal University, Xining 810000, China

³Lanzhou Center for Theoretical Physics, Key Laboratory of Theoretical Physics of Gansu Province, Lanzhou University, Lanzhou, Gansu 730000, China

We study the excited states of ω and ω_3 by comparison with ρ and ρ_3 families, and discuss the possibility of $X(2220)$ as ω excitation by analyzing the mass spectra and strong decay behaviors. In addition, we predict the masses and widths of $\omega(2D)$ and $\omega_3/\rho_3(4D)$, $\omega_3/\rho_3(1G)$, $\omega_3/\rho_3(2G)$ and $\omega_3/\rho_3(3G)$. The abundant information of their two-body strong decays predicted in this work will be helpful to further study of these ω/ω_3 and ρ/ρ_3 states in experiment and theory.

PACS numbers: 14.40.Be, 12.38.Lg, 13.25.Jx

I. INTRODUCTION

Very recently, the BESIII Collaboration announced the observation of the $X(2220)$ state in the $e^+e^- \rightarrow \omega\pi^0\pi^0$ process [1], which has a statistical significance larger than 5σ . The measurement shows that the $X(2220)$ has the mass of $M = 2222 \pm 7 \pm 2$ MeV and the width of $\Gamma = 59 \pm 30 \pm 6$ MeV. It could be an ω excited state from its report. When further checking the experimental status of light mesons, we notice an interesting phenomenon: the states of unflavored light meson families with $J^{PC} = 1^{--}$ and 3^{--} are not established well. In our previous work [2], we carry out an investigation of the mass spectra and Okubo-Zweig-Iizuka allowed two-body strong decay properties of the S -wave and D -wave ω mesons, and make a comparison with the experimental data of these reported ω states and the ω -like $X(2240)$ state observed by BESIII. Now, we reconsider the newly observed $X(2220)$ state and ω/ω_3 , ρ/ρ_3 families.

According to our investigation, we find that there are many scholars has studied ω , ω_3 , ρ and ρ_3 states. As for mesons $J^{PC} = 1^{--}$, In the Ref. [3], $\omega(782)$, $\omega(1420)$ and $\omega(1650)$ are treated as $\omega(1S)$, $\omega(2S)$ and $\omega(1D)$ states, respectively. L.-M. Wang et al. predicted the spectroscopy behavior of ω , ρ and ϕ mesons at the range of $2.4 \sim 3$ GeV [4]. F. Buisseret and C. Semay regard $\omega_3(1670)$ as a 1^3D_3 state [5]. Ebert has calculated masses of the ground state as well as the orbital and radial excited states of quark-antiquark mesons composed of light (u, d, s) quarks within the framework of the relativistic quark model using the quasipotential approach, and concluded that the masses of $\rho_3(1^3D_3)$ and $\omega_3(1^3D_3)$ are 1688.8 MeV and 1667 MeV, respectively. Besides, the masses of other ω and ρ mesons are calculated in Ref. [6]. Anisovich has investigated the Regge trajectory of ρ and ρ_3 , ω and ω_3 mesons and so on [7], which indicates that the states whose masses

are 1700 MeV, 1990 MeV, 2285 MeV as $n = 1$, $n = 2$, $n = 3$ states in the $\rho(IJ^{PC} = 11^{--})$ family, respectively. The masses of 770 MeV, 1450 MeV, 1830 MeV and 2110 MeV states are on the (n, M^2) planes [7]. Lanzhou group has studied ρ , ρ_3 family by assigning $\rho(1700)$, $\rho(2000)$ and $\rho(2270)$ as 1^3D_1 , 2^3D_1 and 3^3D_1 [8], respectively. Besides, $\rho(770)$, $\rho(1450)$, $\rho(1900)$ and $\rho(2150)$ are listed on the line of n^3S_1 . The above result is consist with those in Ref. [9] and Ref. [6].

Similarly, the study on mesons $J^{PC} = 3^{--}$ is a chaotic condition. The states with masses of $M = 1690$ MeV, 1980 MeV and 2300 MeV are on a line of (n, M^2) [7] and the author in Ref. [6] concluded that $\rho_3(1980)$ and $\rho_3(2260)$ can be assigned as $1G_3$ and $2G_3$ states. Besides, $\omega_3(1945)$ was reported by SPEC [10], which also found $\omega_3(2255)$ and $\omega_3(2285)$. The states were later confirmed by RVUE [11]. $\omega_3(1670)$ was suggested to be the ground state of the ω_3 family. Combining the partial wave analysis. (PWA) with the n - M^2 plot, Anisovich, et al. proposed that $\omega_3(1945)$ and $\omega_3(2285)$ are 2^3D_3 and 3^3D_3 states [10], respectively, while $\omega_3(2255)$ is a 3^3G_3 state. Reference [9] suggested that $\omega_3(2285)$ could be the 1^3G_3 state. Calculation of the mass spectra given in Ref. [6] shows that $\omega_3(1945)$ and $\omega_3(2285)$ could be the 1^3G_3 and 2^3G_3 states, respectively.

As an important part of the meson family, the ω/ρ and ω_3/ρ_3 family has become more and more abundant in experiment. BESIII Collaboration reported a result that in the $e^+e^- \rightarrow \omega\pi^0$ cross section, a resonance denoted by $Y(2040)$ is observed recently. Its mass and width are determined to be $2034 \pm 13 \pm 9$ MeV/c² and $234 \pm 30 \pm 25$ MeV/c² [12], respectively. The author in Ref. [13] also treated it as $\rho(2000)$. BESIII Collaboration also reported a state (we call it $X(2239)$) with the mass of $M = 2239.2 \pm 7.1 \pm 11.3$ MeV and the width of $\Gamma = 139.8 \pm 12.3 \pm 20.6$ MeV [14] by studying the cross section of the $e^+e^- \rightarrow K^+K^-$ process. $X(2239)$ is treated as $Y(2175)$ in the Ref. [15]. Reference. [2] assigned $X(2239)$ as the $\omega(4^3S_1)$ state and it is treated $X(2239)$ as the candidate of tetraquark states in Refs. [16, 17]. T. Barnes, S. Godfrey, and E. S. Swanson suggests that further investigation is expected to understand the structures near the $\Lambda\bar{\Lambda}$ threshold, such as $X(2239)$, $\eta(2225)$, and $X(2175)$. However, the properties of $X(2240)$ still remain unclear [18].

In view of the above, a systematic study for the ω , ρ and ω_3 , ρ_3 meson family becomes very necessary and urgent. ω/ω_3

^{*}Corresponding author

[†]Electronic address: nanoshine@foxmail.com

[‡]Electronic address: litingsyan1213@163.com

[§]Electronic address: fang1628671425@163.com

[¶]Electronic address: hchen@qhnu.edu.cn

^{**}Electronic address: pcq@qhnu.edu.cn

and ρ/ρ_3 mesons have same quantum numbers (P and C), for which reason the study of them can be borrowed from each other. We estimate the mass of the missing states in these meson families. Similarly, we study the strong decay of ω/ω_3 meson family comparing with that of ρ/ρ_3 meson family.

In this work, we will study the excited states of ω , ρ and ω_3 , ρ_3 meson. By using MGI model and quark pair creation (QPC) model, the mass spectra and strong decay behavior of the excited states of these mesons are analyzed, which indicates that $X(2220)$ is the candidate of $\omega(3D)$ meson with $I(J^P) = 0(1^-)$. The spectra of the ω , ρ and ω_3 , ρ_3 meson families are studied.

This paper is organized as follows. We first introduce the models applied in this paper **II** and analyze the mass spectra and decay behaviors of ω , ρ and ω_3 , ρ_3 mesons **III**. The paper ends with a summary.

II. MODELS EMPLOYED IN THE WORK

The modified GI quark model, Regge trajectory and the QPC model can be used to calculate the mass spectra and the two-body strong decays of the meson family, respectively. Before discussing the results, the above models will be introduced briefly in the following part.

A. Regge trajectory

Finding the Regge trajectory is an effective approach to study a light-meson spectra [19, 20]. The masses and radial quantum numbers of the light mesons in the same meson family satisfy the following relation:

$$M^2 = M_0^2 + (n-1)\mu^2, \quad (2.1)$$

where M_0 represents the mass of the ground state, μ^2 is the trajectory slope and n is the radial quantum number of the corresponding meson with the mass M .

By analyzing the Regge trajectory, the result demonstrate that $\omega(782)$, $\omega(1420)$ and $\omega(1960)$ are $1S$, $2S$ and $3S$ states, respectively. But the situation of $\omega(4S)$ is not so distinct. All of $\omega(2330)$, $\omega(2290)$ and $X(2240)$ can be the candidate of $\omega(4S)$ because of their approximate masses. The widths of those states are different. The mass of $\omega(2330)$ is larger than that of others, more details can be seen in the Fig. 1. As for D wave, we assign $X(2220)$ and $\omega(2205)$ as the 1^3D_1 state. $\omega_3(1945)$ and $\omega_3(2285)$ are the excited states of $\omega_3(1670)$. $\rho_3(1990)$ and $\rho_3(2250)$ are the $2D$ and $3D$ states, which agrees well with the results in Ref. [8]. We can see the masses of $\omega(1650)$ and $\rho(1700)$, $\omega_3(1670)$ and $\rho_3(1670)$, $\omega_3(1945)$ and $\rho_3(1990)$ are very similar.

B. The modified GI model

In 1985, Godfrey and Isgur proposed the GI model for describing relativistic meson spectra with great success, specifically for low-lying mesons [21]. Regarding the excited states,

the screening potential should be taken into account for its coupled-channel effect [22–25].

The internal interaction of mesons is depicted by the Hamiltonian of the potential model and can be written as

$$\tilde{H} = \sqrt{m_1^2 + \mathbf{p}^2} + \sqrt{m_2^2 + \mathbf{p}^2} + \tilde{V}_{\text{eff}}(\mathbf{p}, \mathbf{r}), \quad (2.2)$$

where m_1 and m_2 denote the mass of quark and antiquark, respectively, the effective potential has a familiar format in the nonrelativistic limit [21, 26]

$$V_{\text{eff}}(r) = H^{\text{conf}} + H^{\text{hyp}} + H^{\text{so}}, \quad (2.3)$$

with

$$H^{\text{conf}} = \left[-\frac{3}{4} \left(\frac{b(1-e^{-\mu r})}{\mu} + c \right) + \frac{\alpha_s(r)}{r} \right] (\mathbf{F}_1 \cdot \mathbf{F}_2) = S(r) + G(r), \quad (2.4)$$

$$H^{\text{hyp}} = -\frac{\alpha_s(r)}{m_1 m_2} \left[\frac{8\pi}{3} \mathbf{S}_1 \cdot \mathbf{S}_2 \delta^3(\mathbf{r}) + \frac{1}{r^3} \left(\frac{3\mathbf{S}_1 \cdot \mathbf{r} \mathbf{S}_2 \cdot \mathbf{r}}{r^2} - \mathbf{S}_1 \cdot \mathbf{S}_2 \right) \right] (\mathbf{F}_1 \cdot \mathbf{F}_2), \quad (2.5)$$

$$H^{\text{so}} = H^{\text{so(cm)}} + H^{\text{so(tp)}}, \quad (2.6)$$

where $\mathbf{S}_1/\mathbf{S}_2$ indicates the spin of quark/antiquark and \mathbf{L} is the orbital momentum. \mathbf{F} are related to the Gell-Mann matrices in color space. For a meson, $\langle \mathbf{F}_1 \cdot \mathbf{F}_2 \rangle = -4/3$, the running coupling constant $\alpha_s(r)$ has the following form:

$$\alpha_s(r) = \sum_k \frac{2\alpha_k}{\sqrt{\pi}} \int_0^{\gamma_k r} e^{-x^2} dx, \quad (2.7)$$

where k is from 1 to 3 and the corresponding α_k and γ_k are two constants, $\alpha_{1,2,3} = 0.25, 0.15, 0.2$ and $\gamma_{1,2,3} = \frac{1}{2}, \frac{\sqrt{10}}{2}, \frac{\sqrt{1000}}{2}$ [21]. The Hamiltonian term H^{conf} consists of two pieces, the spin-independent linear confinement piece $S(r)$ and Coulomb-like potential $G(r)$; H^{hyp} is the color-hyperfine interaction and also includes two parts, tensor and contact terms; H^{so} denotes the spin-orbit interaction with the color magnetic term due to one-gluon exchange and the Thomas precession term, which can be written as

$$H^{\text{so(cm)}} = \frac{-\alpha_s(r)}{r^3} \left(\frac{1}{m_1} + \frac{1}{m_2} \right) \left(\frac{\mathbf{S}_1}{m_1} + \frac{\mathbf{S}_2}{m_2} \right) \cdot \mathbf{L} (\mathbf{F}_1 \cdot \mathbf{F}_2), \quad (2.8)$$

$$H^{\text{so(tp)}} = -\frac{1}{2r} \frac{\partial H^{\text{conf}}}{\partial r} \left(\frac{\mathbf{S}_1}{m_1^2} + \frac{\mathbf{S}_2}{m_2^2} \right) \cdot \mathbf{L}. \quad (2.9)$$

In the light meson system, relativistic effects in effective potential must be considered; the GI model introduces these relativistic effects in two ways.

First, the GI model introduces a smearing function for a $q\bar{q}$ meson, which includes nonlocal interactions and a new form of \mathbf{r} dependence:

$$\rho(\mathbf{r} - \mathbf{r}') = \frac{\sigma^3}{\pi^{3/2}} e^{-\sigma^2(\mathbf{r} - \mathbf{r}')^2}. \quad (2.10)$$

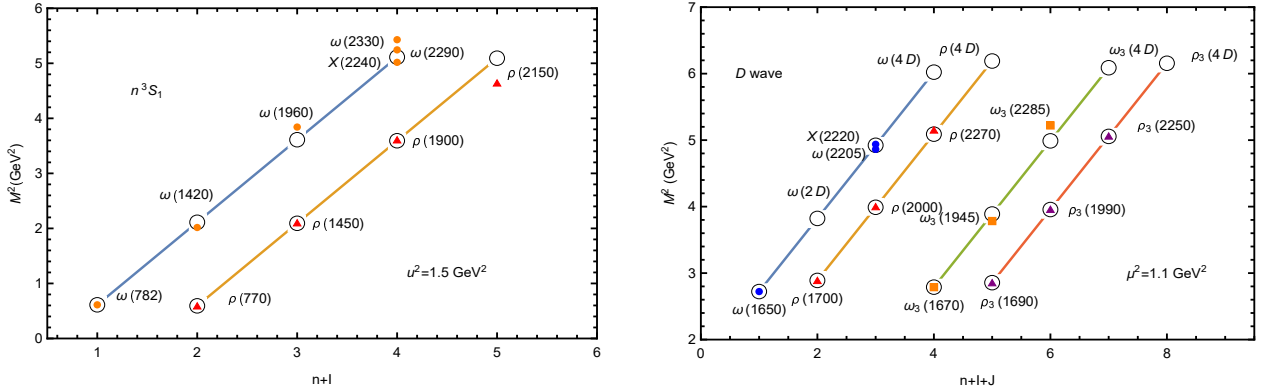


FIG. 1: The S and D waves' Regge trajectories of ω , ω_3 and ρ , ρ_3 families. Here J is the angular momentum of the meson. The open circle and the filled geometry are the theoretical and experimental values, respectively.

Then, $S(r)$ and $G(r)$ become smeared potentials $\tilde{S}(r)$ and $\tilde{G}(r)$, respectively, by the following procedure:

$$\tilde{f}(r) = \int d^3r' \rho(\mathbf{r} - \mathbf{r}') f(r'), \quad (2.11)$$

with

$$\sigma_{12}^2 = \sigma_0^2 \left[\frac{1}{2} + \frac{1}{2} \left(\frac{4m_1 m_2}{(m_1 + m_2)^2} \right)^4 \right] + s^2 \left(\frac{2m_1 m_2}{m_1 + m_2} \right)^2, \quad (2.12)$$

where the values of σ_0 and s are defined in Table I [25].

TABLE I: Parameters and their values in this work, which are determined by fitting the meson experimental data listed in PDG.

Parameter	Value [25]	Parameter	Value [25]
m_u (GeV)	0.163	σ_0 (GeV)	1.799
m_d (GeV)	0.163	s (GeV)	1.497
m_s (GeV)	0.387	μ (GeV)	0.0635
b (GeV 2)	0.221	c (GeV)	-0.240
ϵ_c	-0.138	ϵ_{sov}	0.157
ϵ_{sos}	0.9726	ϵ_t	0.893

Second, to make up for the loss of relativistic effects in the nonrelativistic limit, a general potential relying on the center-of-mass of interacting quarks and momentum are applied as

$$\tilde{G}(r) \rightarrow \left(1 + \frac{p^2}{E_1 E_2} \right)^{1/2} \tilde{G}(r) \left(1 + \frac{p^2}{E_1 E_2} \right)^{1/2}, \quad (2.13)$$

and

$$\frac{\tilde{V}_i(r)}{m_1 m_2} \rightarrow \left(\frac{m_1 m_2}{E_1 E_2} \right)^{1/2+\epsilon_i} \frac{\tilde{V}_i(r)}{m_1 m_2} \left(\frac{m_1 m_2}{E_1 E_2} \right)^{1/2+\epsilon_i}, \quad (2.14)$$

where $\tilde{V}_i(r)$ represents the contact, tensor, vector spin-orbit and scalar spin-orbit terms, and ϵ_i represents the relevant modification parameters as shown in Table I.

Through diagonalizing and solving the Hamiltonian in Eq. (2.2) by exploiting a simple harmonic oscillator (SHO) basis, the mass spectra and wave functions can be obtained. In configuration and momentum space, SHO wave functions have explicit forms:

$$\Psi_{nLM_L}(\mathbf{r}) = R_{nL}(r, \beta) Y_{LM_L}(\Omega_r), \\ \Psi_{nLM_L}(\mathbf{p}) = R_{nL}(p, \beta) Y_{LM_L}(\Omega_p), \quad (2.15)$$

with

$$R_{nL}(r, \beta) = \beta^{3/2} \sqrt{\frac{2n!}{\Gamma(n+L+3/2)}} (\beta r)^L e^{-\frac{r^2 \beta^2}{2}} \\ \times L_n^{L+1/2}(\beta^2 r^2), \quad (2.16)$$

$$R_{nL}(p, \beta) = \frac{(-1)^n (-i)^L}{\beta^{3/2}} e^{-\frac{p^2}{2\beta^2}} \sqrt{\frac{2n!}{\Gamma(n+L+3/2)}} \left(\frac{p}{\beta} \right)^L \\ \times L_n^{L+1/2}\left(\frac{p^2}{\beta^2} \right), \quad (2.17)$$

where $Y_{LM_L}(\Omega)$ is the spherical harmonic function, $L_n^{L+1/2}(x)$ is the associated Laguerre polynomial, and $\beta = 0.4$ GeV for the calculation.

After diagonalization of the Hamiltonian matrix, the mass and wave function of the meson that is available to undergo the strong decay process can be obtained.

C. a brief review of QPC model

The QPC model is used to calculate the hadronic strong decays allowed by OZI rule. This model is firstly proposed by Micu [27] and further developed by Orsay group [28–32]. The QPC model is widely applied to the OZI-allowed two-body strong decays of hadrons in Refs. [3, 8, 24, 25, 33–53].

For the process $A \rightarrow B + C$,

$$\langle BC | \mathcal{T} | A \rangle = \delta^3(\mathbf{P}_B + \mathbf{P}_C) \mathcal{M}^{M_{J_A} M_{J_B} M_{J_C}}, \quad (2.18)$$

where $\mathbf{P}_{B(C)}$ is the three-momentum of a meson $B(C)$ in the rest frame of a meson A . M_{J_i} ($i = A, B, C$) denotes magnetic quantum number. The transition operator \mathcal{T} describes

a quark-antiquark pair which $J^{PC} = 0^{++}$ creation from vacuum. \mathcal{T} can be written as

$$\begin{aligned} \mathcal{T} = & -3\gamma \sum_m \langle 1m; 1 - m | 00 \rangle \int d\mathbf{p}_3 d\mathbf{p}_4 \delta^3(\mathbf{p}_3 + \mathbf{p}_4) \\ & \times \mathcal{Y}_{1m} \left(\frac{\mathbf{p}_3 - \mathbf{p}_4}{2} \right) \chi_{1,-m}^{34} \phi_0^{34} (\omega_0^{34})_{ij} b_{3i}^\dagger(\mathbf{p}_3) d_{4j}^\dagger(\mathbf{p}_4), \end{aligned} \quad (2.19)$$

where the quark and antiquark are denoted by indices 3 and 4, respectively, γ depicts the strength of the creation of $q\bar{q}$ from vacuum, while $\mathcal{Y}_{\ell m}(\mathbf{p}) = |\mathbf{p}|^\ell Y_{\ell m}(\mathbf{p})$ represents the solid harmonics. χ , ϕ , and ω denote the spin, flavor, and color wave functions respectively, which can be treated separately. Subindices i and j denote the color of a $q\bar{q}$ pair. The decay width reads

$$\Gamma = \frac{\pi |\mathbf{P}|}{4 m_A^2} \sum_{J,L} |\mathcal{M}^{JL}(\mathbf{P})|^2, \quad (2.20)$$

where m_A is the mass of an initial state A , and the two decay amplitudes can be related by the Jacob-Wick formula [54] as

$$\begin{aligned} \mathcal{M}^{JL}(\mathbf{P}) = & \frac{\sqrt{4\pi(2L+1)}}{2J_A + 1} \sum_{M_{J_B} M_{J_C}} \langle L0; JM_{J_A} | J_A M_{J_A} \rangle \\ & \times \langle J_B M_{J_B}; J_C M_{J_C} | J_A M_{J_A} \rangle \mathcal{M}^{M_{J_A} M_{J_B} M_{J_C}}. \end{aligned} \quad (2.21)$$

In calculation, the spatial wave functions of the discussed mesons can be numerically obtained by MG model.

III. NUMERICAL RESULTS AND PHENOMENOLOGICAL ANALYSIS

A. Mass spectra analysis

Applying the MG model and the parameters in Table I, the mass spectra of the ω , ρ and ω_3 , ρ_3 families can be obtained and are shown in Table II, Table III and Table IV. By calculated, The mass spectra of S wave and D wave of ω and ρ mesons as well as ω_3 and ρ_3 mesons are showed in the Table II, Table III and Table IV. We find that the lower energy excited states such as $1S$, $2S$ and $1D$, $2D$ are consist with experimental values [55, 56].

As for ω_3 and ρ_3 meson families, there is too little information to help us determine their structure. For the states of D wave, $\omega_3(1670)$ and $\rho_3(1690)$ are the $1D$ states which has been certified by many scholars [5, 6, 9, 57]. With respect to $2D$ states, we predict the mass of $\omega(2D)$ and $\rho(2D)$ are both 2074 MeV. At the same time, $\rho(2000)$ is a $\rho(2D)$ state [8, 9], which is also close to the theoretical prediction. With regard to $3D$ states of ω_3 and ρ_3 , the value of the mass that we calculated is 2376.5 MeV. Moreover, we consider $\rho_3(2250)$ as the $\rho_3(3D)$ state, which agree well with the result in Ref. [8].

Besides, we have also calculated the mass spectra of ω_3 and ρ_3 of G wave. The masses of $1G$, $2G$ and $3G$ are 2254.8 MeV, 2522.3 MeV and 2748.5, respectively. We hope that these information can help find these resonances from experiment.

B. DECAY MODES AND WIDTH

ω/ω_3 and ρ/ρ_3 mesons have the same quantum numbers(P and C), for which reason the study of them can be learned from each other. We estimate the mass of the missing states in these meson families. Similarly, we study the strong decay of ω/ω_3 meson family comparing with that of ρ/ρ_3 meson family. The γ value in Eq. (2.19) is taken by the following method. When fitting the ρ/ρ_3 meson experimental width value (with error) using the theoretical total width, the range of γ value can be fixed. Then we use this γ value to calculate the width of ω/ω_3 meson. Some decay channels which less than 1 MeV are omitted.

1. S -wave ω and ρ mesons

By analyzing the above masses of ω and ρ states, we know that $\omega(1420)$, $\omega(1960)$, $\omega(2330)$, $\omega(2290)$ and $X(2240)$ are the radial excitations of $\omega(782)$. $\rho(1450)$, $\rho(1900)$ and $\rho(2150)$ are the $\rho(2S)$, $\rho(3S)$ and $\rho(4S)$ states respectively. We will then discuss these states.

From TABLE V, $\omega(1420)$ dominantly decay into $\rho\pi$ which is consist with experiment [64] and Ref. [65]. $\eta\rho$, KK , $b_1\pi$ and KK^* are the main decay modes in which $b_1\pi$ was observed in experiment [64]. The total width of $\omega(1420)$ in our calculation has a overlap with the experiment value [58]. $\omega(1420)$ is a good candidate of $\omega(2S)$ which agree with Ref. [3].

TABLE VI: The total and partial decay widths of the $\omega(3S)$ and $\rho(3S)$, the unit of widths is MeV. The γ value is 6.3-7.9.

$\omega(1960)$, $\Gamma_{exp.} = 195 \pm 60$ [10]		$\rho(1900)$, $\Gamma_{exp.} = 130 \pm 30$ [64]	
Channel	Value	Channel	Value
Total	191 ± 42.5	Total	130
$\rho\pi$	108	$a_2\pi$	31.1
$b_1\pi$	32.0	$\omega\pi$	29.2
KK_1	14.8	KK_1	18.7
$\eta\omega$	9.90	$\pi\pi(1300)$	16.1
$KK^*(1410)$	9.40	$\pi\pi$	13.9
$h_1\eta$	4.74	$a_1\pi$	13.0
KK^*	3.77	KK	2.60
KK	3.14	$b_1\eta$	2.55
KK'_1	2.35	KK^*	2.46

$\omega(1960)$ is observed in the $p\bar{p} \rightarrow \omega\eta$, and $\omega\pi\pi$ process [10]. As shown in TABLE VI, $\omega(1960)$ dominantly decay into $\rho\pi$ under $\omega(3S)$ assignment. The decay modes $b_1\pi$, KK_1 and KK' make some contribution to the total width, and $b_1\pi$ can decay to $\omega\pi\pi$ which is the final channel observed in experiment [10]. According to our calculation, the total width of $\omega(1960)$ is 191.1 ± 42.5 MeV and this is consistent with the experimental data [10]. In addition, $\omega\eta$ is a sizable final channel and has been observed in experiment [10]. Other detailed

TABLE II: The mass spectrum of S wave of ω and ρ mesons. "Expe." represents experimental value. The unit of the mass is MeV.

	1 S	2 S	3 S	4 S			5 S
ω	mass in MGI	773.8	1424.3	1906.1		2259.1	2542.1
	ω states	$\omega(782)$	$\omega(1420)$	$\omega(1960)$	$\omega(2330)$	$\omega(2290)$	$X(2240)$
	Expe. mass	782.65 ± 0.12 [55]	1410 ± 60 [55]	1960 ± 25 [55]	2330 ± 30 [55]	2290 ± 20 [55]	$2239.2 \pm 7.1 \pm 11.3$ [14]
	Expe. width	8.49 ± 0.08 [55]	880 ± 170 [58]	195 ± 60 [10]	435 ± 75 [55]	275 ± 35 [55]	$139.8 \pm 12.3 \pm 20.6$ [14]
ρ	ρ states	$\rho(770)$	$\rho(1450)$	$\rho(1900)$		$\rho(2150)$	--
	Expe. mass	775.26 ± 0.25 [55]	1465 ± 25 [55]	1909 ± 30.2 [59]		2201 ± 19 [60]	--
	Expe. width	147.8 ± 0.9 [55]	400 ± 6 [55]	130 ± 30 [61]		310 ± 140 [62]	--

TABLE III: The mass spectrum of D wave of ω and ρ mesons. "Expe." represents experimental value. The unit of the mass is MeV.

	1 D	2 D	3 D	4 D	
ω	mass in MGI	1646.2	2047.6	2365.0	2624.0
	ω states	$\omega(1650)$	$\omega(2D)$	$\omega(2205)$	$X(2220)$
	Expe. mass	1670 ± 30 [55]	--	2205 ± 30 [55]	2222 ± 7.3 [1]
	Expe. width	315 ± 35 [55]	--	350 ± 90 [55]	59 ± 30.6 [1]
ρ	ρ states	$\rho(1700)$	$\rho(2000)$	$\rho(2270)$	$\rho(4D)$
	Expe. mass	1720 ± 20 [55]	2000 ± 30 [56]	2265 ± 40 [55]	--
	Expe. width	250 ± 100 [55]	260 ± 45 [56]	325 ± 80 [55]	--

information is demonstrated in TABLE VI. Our calculation indicates that $\omega(1960)$ can be assigned as $\omega(3S)$ state.

$X(2240)$ is observed in the $e^+e^- \rightarrow K^+K^-$ process by the BESIII Collaboration, which has the mass of $2239.2 \pm 7.1 \pm 11.3$ MeV and the width of $139.8 \pm 12.3 \pm 20.6$ MeV [14]. The quantum number of this resonant structure can be assigned as $J^{PC} = 1^{--}$. Assuming that it is a isospin scalar state, it may be a $\omega(4S)$ candidate from our previous mass analysis. The new state $X(2240)$ needs more theoretical and experimental research to recover its structure. $\omega(2330)$ is firstly observed in the $\gamma p \rightarrow \rho^\pm \rho^0 \pi^\pm$ process [66]. It has the mass of 1330 ± 30 MeV and the width of 435 ± 75 MeV. $\omega(2290)$ is reported in the partial wave analysis of the data on $p\bar{p} \rightarrow \bar{\Lambda}\Lambda$ [11], which has the mass of 2290 ± 20 MeV and the width of 275 ± 35 MeV. $\omega(2330)$, $\omega(2290)$ and $X(2240)$ are the candidates of the $\omega(4S)$ according to our calculation and the obtained widths are in good agreement with experimental values. $\rho(1450)\pi$ is the primary decay mode of $\omega(2330)$, $X(2240)$ and $\omega(2290)$ if assign them as $\omega(4S)$ states. Besides, $b_1\pi$, $a_1\rho$ and $\rho\pi$ make needful contribution to the total width of $\omega(4S)$, other decay modes contribute less to the total width as shown in TABLE VII.

As for S wave state of ρ family, we assign $\rho(1450)$, $\rho(1900)$ and $\rho(2150)$ as $\rho(2S)$, $\rho(3S)$ and $\rho(4S)$ states, which consists with the result of Ref. [8]. When $\rho(1450)$ is treated as the $\rho(2S)$, $\omega\pi$ and $\eta\rho$ are predicted to be its important decay channels. KK , $\pi\pi$ and KK^* are the sizable decay modes as well. $\rho(1900)$ is a good candidate of $\rho(3S)$. As shown in the second column of TABLE VI, the decay modes of $\rho(1900)$ are predicted. $a_2\pi$, KK_1 and $\omega\pi$ are its dominant decay modes.

$\pi\pi$, $\pi\pi(1300)$ and $a_1\pi$ are the important final states. We assign $\rho(2150)$ as $\rho(4S)$ based on our calculation. The channels $\pi\omega_3$, $a_2(1700)\pi$, $\pi\pi(1300)$ and $\pi\omega$ are the main channels. Otherwise, $a_2(1320)\pi$, $\pi\pi(1800)$, $h_1(1170)\pi$ and $a_1(1260)\pi$ have sizable contributions to the total width of $\rho(4S)$.

2. D-wave ω and ρ mesons

In this section, we will give an analysis for the D-wave ω and ρ mesons by the means of their two-body strong decay behaviour.

$\omega(1650)$ is well established as a 1D state in the ω family in theory [2, 3, 64], and its main decay channel is $b_1\pi$, whose branch ratio is about 0.8. $\rho\pi$, KK , $\eta\omega$ and KK^* are the important modes. $\rho(1700)$ is a good candidate of the 1^3D_1 ρ meson. The analysis of $\rho(1700) \rightarrow 2\pi, 4\pi$ [67] and the study of $e^+e^- \rightarrow \omega\pi^0$ via the nonrelativistic 3P_0 quark model [68] both indicate that $\rho(1700)$ is a 1^3D_1 state. $\rho(1700)$ mainly decays into $a_1\pi$, $h_1\pi$ and $\rho\rho$ with branch ratios being about 0.38, 0.34 and 0.11, respectively.

TABLE IV: The mass spectra of D wave of ω_3 and ρ_3 mesons. "Expe." represents experimental value. The unit of the mass and width are MeV.

D wave	1 D	2 D	3 D	4 D
mass in MGI	1708.2	2074.0	2376.5	2628.8
ω_3 states	$\omega_3(1670)$	$\omega_3(1945)$	$\omega_3(2285)$	--
Expe. mass	1667 \pm 4 [55]	1945 \pm 20 [55]	2285 \pm 60 [55]	--
Expe. width	168 \pm 10 [55]	115 \pm 22 [55]	230 \pm 40 [55]	--
ρ_3 states	$\rho_3(1690)$	$\rho_3(1990)$	$\rho_3(2250)$	--
Expe. mass	1688.8 \pm 2.1 [55]	1982 \pm 14 [55]	2232 [55]	--
Expe. width	161 \pm 10 [55]	188 \pm 24 [55]	135 \pm 75 [63]	--
G wave	1 G	2 G	3 G	
mass in MGI	2254.8	2522.3	2748.5	
Expe. mass	2255 \pm 15 [55]	--	--	
Expe. width	175 \pm 30 [55]	--	--	

TABLE V: The total and partial decay widths of the $\omega(2S)$ and $\rho(2S)$, the unit of widths is MeV. The γ value is 11.5-13.4.

$\omega(1420)$, $\Gamma_{exp.} = 880 \pm 170$ [58]			$\rho(1450)$, $\Gamma_{exp.} = 400 \pm 60$ [64]		
Channel	Value	Ref. [65]	Channel	Value	Ref. [65]
Total	690 \pm 105	378	Total	400	279
$\rho\pi$	608	328	$\omega\pi$	220	122
$\eta\rho$	33.3		$\eta\rho$	58.0	
KK	28.3	31	KK	31.9	
$b_1\pi$	12.1	1	$\pi\pi$	30.9	74
KK^*	9.50	5	KK^*	30.3	
			$a_1\pi$	14.9	3
			$h_1\pi$	9.05	1

TABLE IX: The total and partial decay widths of the $\omega(2D)$ and $\rho(2D)$, the unit of widths is MeV. The γ value is 5.4-6.4.

$\omega(2D)$		$\rho(2000)$, $\Gamma = 260 \pm 45$ [64]	
Channel	Value	Channel	Value
Total	212 \pm 36.1	Total	260
$b_1\pi$	110	$a_1(1640)\pi$	58.4
$\pi\rho(1450)$	24.7	πh_1	36.6
$\pi\rho$	22.7	$\rho\rho$	35.2
ρa_1	22.1	$\pi\pi_2$	34.1
ηh_1	13.2	πa_1	26.3
$KK^*(1410)$	4.29	$\pi\pi$	21.9
$\eta\omega(1420)$	3.26	$\pi\pi(1300)$	19.8
$\eta\omega$	2.60	$\pi\omega(1420)$	8.22
KK	2.18	$\pi\omega$	6.39
KK_1	1.83	ηb_1	4.50
KK^*	1.15	$KK^*(1410)$	2.54
		KK	1.81
		$\eta\rho$	1.70

As is shown in Fig. 1 and TABLE III, the mass of $\omega(2D)$ is predicted, which is still unobserved. $\omega(2D)$ has the total width of about 211.85 ± 36.05 MeV. $b_1\pi$ is its dominant decay channel, whose branch ratio is 0.5. $\pi\rho(1450)$, $\pi\rho$ and ρa_1 are its important decay channels and more details can be seen in TABLE IX. We suggest that experimentalists focus on these final channel. In 1994, a resonance around 1988 MeV was found in $\bar{p}p \rightarrow \pi\pi$ from 0.36 to 2.5 GeV reaction. Later in 2011, A.V. Anisovich et al. found a resonance that $J^{PC} = 1^{--}$ and its mass is of 2000 ± 30 MeV. $\rho(2000)$ is treated as $\rho(2D)$ state. $a_1(1640)\pi$, πh_1 , $\rho\rho$ and $\pi\pi_2(1670)$ have sizable contributions to the total width of $\rho(2D)$.

$X(2220)$ state is found in the $e^+e^- \rightarrow \omega\pi^0\pi^0$ process [1],

which has the mass of $M = 2222 \pm 7 \pm 2$ MeV and the width of $\Gamma = 59 \pm 30 \pm 6$ MeV. $X(2220)$ is an excellent candidate of $\omega(3D)$ by Regge trajectory analysis and according to TABLE X. When $X(2220)$ is treated as the $\omega(3D)$ state, its width is close to the experiment value. $\omega(2205)$ is also assigned as $\omega(3D)$ state based on mass spectra analysis. $b_1\pi$ is the main decay mode of $\omega(3D)$. $\pi\rho(1450)$ and ρa_1 are the important decay channels of $\omega(3D)$, other modes like $KK_1(1270)$, ρa_2 , $\pi\rho$ and so on also have contribution to the total width of $\omega(3D)$, more details can be seen in TABLE X.

3. D-wave ω_3 and ρ_3 mesons

Referring to PDG, we can find some experimental results about ω_3 and ρ_3 , which are $\rho_3(1690)$, $\rho_3(1990)$, $\rho_3(2250)$, $\omega_3(1670)$, $\omega_3(1945)$, $\omega_3(2285)$ and $\omega_3(2255)$. We carry out an investigation of the Okubo-Zweig-Iizuka allowed a two-body strong decay of the D-wave and G-wave ω_3 / ρ_3 mesons.

There exists a lot of data for $\omega_3(1670)$ from PDG. D.V. Amelin et al. first found it in the $\pi^- p \rightarrow \pi^+ \pi^- \pi^0 n$ reactions, which has the mass of $1665.3 \pm 5.2 \pm 4.5$ MeV [70]. and then C. Baltay, C. V. Cautis and M. Kalelkar reported the existence of a high-mass, $I = 0$ resonant state with odd G parity, whose mass and width are $M = 1.63 \pm 0.012$ GeV and $\Gamma = 0.173 \pm 0.016$ GeV, respectively. At present, $\omega_3(1670)$ is established to be a 1^3D_3 state. $\pi\rho$ is the main decay modes of $\omega_3(1D)$, which has the branch ratios of 0.77. Additionally, $b_1\pi$, $\eta\omega$, KK , KK^* and $\pi\rho(1450)$ also make contribution to the total width of $\omega_3(1D)$.

The $\omega_3(1670)$ state was first found in the $\pi^+ n \rightarrow p 3\pi^0$ process [71] and has been studied by other experiments (the details for the experimental information on $\omega_3(1670)$ are listed in the Particle Data Group (PDG) [72]). $\omega_3(1670)$ can decay into $\rho\pi$ and $\pi\omega\pi$ according to Ref. [57]. From our study, $\omega_3(1670)$ decay into $\pi\rho$, $b_1\pi$, $\eta\omega$ and KK when treated as $\omega_3(1D)$ state. $\rho_3(1690)$ is well established to be a 1^3D_3 state, which decay into $\rho\rho$, $\pi\pi$, $\pi\omega$ and πh_1 as shown in TABLE XI and the branch ratios are about 0.55, 0.17, 0.12 and 0.056, respectively.

$\omega_3(1945)$ was firstly observed in the $p\bar{p} \rightarrow \omega\eta, \omega\pi^0\pi^0$ [73]. it has the mass of 1945 ± 20 MeV and the width of 115 ± 22 MeV. We assign it as $\omega_3(2D)$ state and calculated the two-body strong decay as shown in TABLE XII. We see from TABLE XII that $b_1\pi$, $\pi\rho$, $\pi\rho(1450)$ and $\rho_3(1690)\pi$ are major decay modes of $\omega_3(2D)$. $\eta\omega$, $h_1\eta$, K^*K^* and KK^* are important channels. When treated as $\rho_3(2D)$, $\rho_3(1990)$ mainly decay into $\pi\pi(1300)$, $\pi a_2(1320)$, $\rho\rho$, which branch ratios are 0.22, 0.18 and 0.14, respectively. Besides, $\rho_3(1990) \rightarrow \pi a_1(1260)$, $\pi h_1(1170)$, $\pi\omega(1420)$ are sizeable. More details can be seen in TABLE XI.

As for $\omega_3(3D)$, we consider $\omega_3(2285)$ is the best candidate according to the mass spectra analysis and we give its decay modes and values in TABLE XIII. The total width of $\omega_3(2285)$ is 226 ± 126 MeV if we treat $\omega_3(2285)$ as a $\omega_3(3D)$ state. $a_2\rho$, $\pi\rho$, $f_2\omega$ and $b_1\pi$ make great contribution to its total width and $\rho_3(1690)\pi$, $\pi(1300)\rho$, $\pi\rho(1450)$ and so forth are also important decay channels. Meanwhile, $\rho_3(2250)$ is established to be a

$\rho_3(3D)$ state, which can decay into ωa_2 , ρf_2 , $\pi\omega$, $\rho\rho$ as shown in TABLE XIII.

$\omega_3(4D)$ and $\rho_3(4D)$ are still missing in experiment. We calculated the width of $\omega_3(4D)$ is about 290 MeV and $\rho_3(4D)$ is approximately 420 MeV. According to TABLE XIV, the main decay modes of $\omega_3(4D)$ are $a_2\rho$, $\pi(1300)\rho$, $b_1\pi$ and $\pi\rho$. $\rho_3(4D)$ mainly decay into ωa_2 , ρf_2 , $\pi\omega$ and so on. These predictions can help us search for $\omega_3(4D)$ and $\rho_3(4D)$ states.

4. G-wave ρ_3 and ω_3 mesons

According to Tale XV, $b_1\pi$, $\rho_3\pi$ and $h_1\eta$ are predicted to be $\omega_3(1G)$'s important decay channels, which have the ratios of 0.45, 0.14 and 0.1, respectively. We suggest that experimentalists focus on these final channels. The total width of $\omega_3(1G)$ is 325 MeV. The total width of $\rho_3(1G)$ is approximately 721 MeV. $\pi_2\pi$, $b_1\rho$, $\rho\rho$ and $a_1\pi$ are its important decay channels. Considering the final decay channels, $\pi_2\pi$ will be the most important final channels in searching for $\rho_3(1G)$ state experimentally. More details can be seen in Tale XV. Thes predictions can help us search for and establish $\omega_3(1G)/\rho_3(1G)$ state.

The decay information of the $\omega_3(2G)/\rho_3(2G)$ is listed in Table XVI. As shown in the first column of Table XVI, the strong decay of $\omega_3(2G)$ is predicted, which is still unobserved. $\omega_3(2G)$ has the total width of 312 MeV. $b_1\pi$ is its dominant decay channel, which ratios is 0.34. $a_2\rho$, $\pi_2\rho$, $\rho_3\pi$, $h_1\eta$ and $\pi\rho$ are the important final states. η' , $a_1\rho$ and $h_1\eta'$ are small. The total width of $\rho_3(2G)$ is 397 MeV. $\rho_3(2G) \rightarrow \pi_2\pi$ will be the dominant decay mode. In the calculation, $h_1\pi$, $a_1\pi$ and $\rho\rho(1450)$ are the important decay channels. Other decay information can be seen in Table XVI.

The decay information of the $\omega_3/\rho_3(3G)$ are also predicted in this work. The total width of $\omega_3(3G)$ is approximately 181 MeV. The channels $b_1\pi$, $\pi\rho$, $\rho_3\pi$ and $f_1\omega$ have the branch ratios of 0.35, 0.07, 0.07 and 0.06, respectively, which are the main decay modes. $\pi_2\rho$, $h_1\eta$, $b_1\pi(1300)$ and $f_2\omega$ are its important decay channels. This work suggests that experimentlist should search for this missing state in $b_1\pi$ final state. Otherwise, $\pi(1300)\rho$, $a_2\rho$, $\pi\rho(1450)$, $a_0\rho$ and $h_1\eta(1295)$ have sizeable contributions to the total width of $\omega_3(3G)$. $\rho_3(3G)$ has the total width of about 270 MeV from our calculation. The main decay modes are $\pi_2\pi$, $\rho\rho$, $h_1\pi$, $a_1\omega$ and $a_1\pi$, which branch ratios are 0.17, 0.090, 0.089, 0.086 and 0.078. $a_2\pi$, $a_2(1700)\pi$, $f_2\rho$, $\rho\eta(1295)$ and $\rho\rho(1450)$ are the important decay modes of $\rho_3(3G)$.

IV. CONCLUSION

In this work, we have systematically studied the mass spectra and the OZI-allowed two-body strong decay behaviors of the newly observed $X(2220)$ state as well as ω/ω_3 and ρ/ρ_3 states. We adopt a new way to get the value of γ in ω/ω_3 system. Following is the main work.

1. The newly observed state $X(2220)$ should be a 3^3D_1 ω state.

2. The $\omega(782)$, $\omega(1420)$ and $\omega(1960)$ states can be interpreted as the $\omega(1^3D_1)$, $\omega(2^3D_1)$ and $\omega(3^3D_1)$. All of $\omega(2240)$, $\omega(2330)$ and $\omega(2290)$ can be the candidate of $\omega(4^3D_1)$. $\rho(1450)$, $\rho(1900)$ and $\rho(2150)$ are the first, second and third excited states of $\rho(770)$ as shown in Fig. 1.
3. The mass and width of $\omega(2D)$, by our prediction, are 2047.6 MeV and 212 ± 36.1 MeV. $\omega(2205)$ and $X(2220)$ are the $\omega(3D)$ states.
4. $\omega_3(1945)$, $\omega_3(2285)$ and $\rho_3(1990)$, $\rho_3(2250)$ are the first and second excited states of $\omega_3(1670)$ and $\rho_3(1690)$.
5. We predict the masses of $\omega_3(4D)$ and $\rho_3(4D)$ are both 2.63 GeV, the width of them are 288 MeV and 420

MeV. We also predict the mass spectrums and decay behaviors of $\omega_3(1G)/\rho_3(1G)$, $\omega_3(2G)/\rho_3(2G)$ and $\omega_3(3G)/\rho_3(3G)$.

In addition, it is our hope and belief that more experimental measurements will be released in the future.

V. ACKNOWLEDGE

This work is supported by the National Natural Science Foundation of China under Grants No. 11965016 and Department of Qinghai Province No. 2020-ZJ-728.

[1] M. Ablikim et al. (BESIII), *Phys. Rev. D* **105**, 032005 (2022), [arXiv:2112.15076 \[hep-ex\]](https://arxiv.org/abs/2112.15076) .

[2] C.-Q. Pang, Y.-R. Wang, J.-F. Hu, T.-J. Zhang, and X. Liu, *Phys. Rev. D* **101**, 074022 (2020), [arXiv:1910.12408 \[hep-ph\]](https://arxiv.org/abs/1910.12408) .

[3] X. Wang, Z.-F. Sun, D.-Y. Chen, X. Liu, and T. Matsuki, *Phys. Rev. D* **85**, 074024 (2012), [arXiv:1202.4139 \[hep-ph\]](https://arxiv.org/abs/1202.4139) .

[4] L.-M. Wang, S.-Q. Luo, and X. Liu, (2021), [arXiv:2109.06617 \[hep-ph\]](https://arxiv.org/abs/2109.06617) .

[5] F. Buisseret and C. Semay, *Phys. Rev. D* **71**, 034019 (2005), [arXiv:hep-ph/0412361 \[hep-ph\]](https://arxiv.org/abs/hep-ph/0412361) .

[6] D. Ebert, R. Faustov, and V. Galkin, *Phys. Rev. D* **79**, 114029 (2009), [arXiv:0903.5183 \[hep-ph\]](https://arxiv.org/abs/0903.5183) .

[7] V. V. Anisovich, American Institute of Physics (2004).

[8] L.-P. He, X. Wang, and X. Liu, *Phys. Rev. D* **88**, 034008 (2013), [arXiv:1306.5562 \[hep-ph\]](https://arxiv.org/abs/1306.5562) .

[9] S. Afonin, *Phys. Rev. C* **76**, 015202 (2007), [arXiv:0707.0824 \[hep-ph\]](https://arxiv.org/abs/0707.0824) .

[10] A. Anisovich, C. Baker, C. Batty, D. Bugg, L. Montanet, et al., *Phys. Lett. B* **542**, 19 (2002), [arXiv:1109.5817 \[hep-ex\]](https://arxiv.org/abs/1109.5817) .

[11] D. Bugg, *Eur. Phys. J. C* **36**, 161 (2004), [arXiv:hep-ph/0406292 \[hep-ph\]](https://arxiv.org/abs/hep-ph/0406292) .

[12] M. Ablikim et al. (BESIII), *Phys. Lett. B* **813**, 136059 (2021), [arXiv:2009.08099 \[hep-ex\]](https://arxiv.org/abs/2009.08099) .

[13] Z.-Y. Li, D.-M. Li, E. Wang, W.-C. Yan, and Q.-T. Song, (2021), [arXiv:2102.05356 \[hep-ph\]](https://arxiv.org/abs/2102.05356) .

[14] M. Ablikim et al. (BESIII), *Phys. Rev. D* **99**, 032001 (2019), [arXiv:1811.08742 \[hep-ex\]](https://arxiv.org/abs/1811.08742) .

[15] D.-Y. Chen, J. Liu, and J. He, *Phys. Rev. D* **101**, 074045 (2020), [arXiv:2004.09701 \[hep-ph\]](https://arxiv.org/abs/2004.09701) .

[16] Q.-F. Lü, K.-L. Wang, and Y.-B. Dong, *Chinese Physics C* **44**, 024101 (2020).

[17] K. Azizi, S. S. Agaev, and H. Sundu, *Nucl. Phys. B* **948**, 114789 (2019), [arXiv:1906.04061 \[hep-ph\]](https://arxiv.org/abs/1906.04061) .

[18] J.-T. Zhu, Y. Liu, D.-Y. Chen, L. Jiang, and J. He, *Chin. Phys. C* **44**, 123103 (2020), [arXiv:1911.03706 \[hep-ph\]](https://arxiv.org/abs/1911.03706) .

[19] G. F. Chew and S. C. Frautschi, *Phys. Rev. Lett.* **8**, 41 (1962).

[20] A. Anisovich, V. Anisovich, and A. Sarantsev, *Phys. Rev. D* **62**, 051502 (2000), [arXiv:hep-ph/0003113 \[hep-ph\]](https://arxiv.org/abs/hep-ph/0003113) .

[21] S. Godfrey and N. Isgur, *Phys. Rev. D* **32**, 189 (1985).

[22] Q.-T. Song, D.-Y. Chen, X. Liu, and T. Matsuki, *Phys. Rev. D* **91**, 054031 (2015), [arXiv:1501.03575 \[hep-ph\]](https://arxiv.org/abs/1501.03575) .

[23] Q.-T. Song, D.-Y. Chen, X. Liu, and T. Matsuki, *Phys. Rev. D* **92**, 074011 (2015), [arXiv:1503.05728 \[hep-ph\]](https://arxiv.org/abs/1503.05728) .

[24] C.-Q. Pang, J.-Z. Wang, X. Liu, and T. Matsuki, *Eur. Phys. J. C* **77**, 861 (2017), [arXiv:1705.03144 \[hep-ph\]](https://arxiv.org/abs/1705.03144) .

[25] C.-Q. Pang, Y.-R. Wang, and C.-H. Wang, *Phys. Rev. D* **99**, 014022 (2019), [arXiv:1810.02694 \[hep-ph\]](https://arxiv.org/abs/1810.02694) .

[26] W. Lucha, F. F. Schoberl, and D. Gromes, *Phys. Rept.* **200**, 127 (1991).

[27] L. Micu, *Nucl. Phys. B* **10**, 521 (1969).

[28] A. Le Yaouanc, L. Oliver, O. Pene, and J. Raynal, *Phys. Rev. D* **8**, 2223 (1973).

[29] A. Le Yaouanc, L. Oliver, O. Pene, and J.-C. Raynal, *Phys. Rev. D* **9**, 1415 (1974).

[30] A. Le Yaouanc, L. Oliver, O. Pene, and J. Raynal, *Phys. Rev. D* **11**, 1272 (1975).

[31] A. Le Yaouanc, L. Oliver, O. Pene, and J. Raynal, *Phys. Lett. B* **72**, 57 (1977).

[32] A. Le Yaouanc, L. Oliver, O. Pene, and J.-C. Raynal, *Phys. Lett. B* **71**, 397 (1977).

[33] E. van Beveren, C. Dullemond, and G. Rupp, *Phys. Rev. D* **21**, 772 (1980), [Erratum: *Phys. Rev. D* **22**, 787 (1980)].

[34] E. van Beveren, G. Rupp, T. Rijken, and C. Dullemond, *Phys. Rev. D* **27**, 1527 (1983).

[35] S. Capstick and W. Roberts, *Phys. Rev. D* **49**, 4570 (1994), [arXiv:nucl-th/9310030 \[nucl-th\]](https://arxiv.org/abs/nucl-th/9310030) .

[36] P. R. Page, *Nucl. Phys. B* **446**, 189 (1995), [arXiv:hep-ph/9502204 \[hep-ph\]](https://arxiv.org/abs/hep-ph/9502204) .

[37] A. I. Titov, T. I. Gulamov, and B. Kampfer, *Phys. Rev. D* **53**, 3770 (1996).

[38] E. Ackleh, T. Barnes, and E. Swanson, *Phys. Rev. D* **54**, 6811 (1996), [arXiv:hep-ph/9604355 \[hep-ph\]](https://arxiv.org/abs/hep-ph/9604355) .

[39] H. G. Blundell, [hep-ph/9608473](https://arxiv.org/abs/hep-ph/9608473) (1996).

[40] R. Bonnaz, B. Silvestre-Brac, and C. Gignoux, *Eur. Phys. J. A* **13**, 363 (2002), [arXiv:hep-ph/0101112 \[hep-ph\]](https://arxiv.org/abs/hep-ph/0101112) .

[41] H. Q. Zhou, R. G. Ping, and B. S. Zou, *Phys. Lett. B* **611**, 123 (2005), [arXiv:hep-ph/0412221 \[hep-ph\]](https://arxiv.org/abs/hep-ph/0412221) .

[42] J. Lu, X.-L. Chen, W.-Z. Deng, and S.-L. Zhu, *Phys. Rev. D* **73**, 054012 (2006), [arXiv:hep-ph/0602167 \[hep-ph\]](https://arxiv.org/abs/hep-ph/0602167) .

[43] B. Zhang, X. Liu, W.-Z. Deng, and S.-L. Zhu, *Eur.Phys.J. C50*, 617 (2007), arXiv:hep-ph/0609013 [hep-ph].

[44] Z.-G. Luo, X.-L. Chen, and X. Liu, *Phys. Rev. D79*, 074020 (2009), arXiv:0901.0505 [hep-ph].

[45] Z.-F. Sun and X. Liu, *Phys.Rev. D80*, 074037 (2009), arXiv:0909.1658 [hep-ph].

[46] X. Liu, Z.-G. Luo, and Z.-F. Sun, *Phys.Rev.Lett. 104*, 122001 (2010), arXiv:0911.3694 [hep-ph].

[47] Z.-F. Sun, J.-S. Yu, X. Liu, and T. Matsuki, *Phys.Rev. D82*, 111501 (2010), arXiv:1008.3120 [hep-ph].

[48] T. Rijken, M. Nagels, and Y. Yamamoto, *Nucl.Phys. A835*, 160 (2010).

[49] Z.-C. Ye, X. Wang, X. Liu, and Q. Zhao, *Phys.Rev. D86*, 054025 (2012), arXiv:1206.0097 [hep-ph].

[50] Y. Sun, X. Liu, and T. Matsuki, *Phys.Rev. D88*, 094020 (2013), arXiv:1309.2203 [hep-ph].

[51] C.-Q. Pang, L.-P. He, X. Liu, and T. Matsuki, *Phys. Rev. D90*, 014001 (2014), arXiv:1405.3189 [hep-ph].

[52] B. Wang, C.-Q. Pang, X. Liu, and T. Matsuki, *Phys. Rev. D91*, 014025 (2015), arXiv:1410.3930 [hep-ph].

[53] K. Chen, C.-Q. Pang, X. Liu, and T. Matsuki, *Phys. Rev. D91*, 074025 (2015), arXiv:1501.07766 [hep-ph].

[54] M. Jacob and G. Wick, *Annals Phys. 7*, 404 (1959).

[55] P. A. Zyla *et al.* (Particle Data Group), *PTEP* **2020**, 083C01 (2020).

[56] D. V. Bugg, *Physics Reports* **397**, 257 (2004).

[57] C.-Q. Pang, B. Wang, X. Liu, and T. Matsuki, *Phys. Rev. D92*, 014012 (2015), arXiv:1505.04105 [hep-ph].

[58] V. M. Aul'chenko *et al.*, *J. Exp. Theor. Phys. 121*, 27 (2015), [Zh. Eksp. Teor. Fiz. 148,no.1,34(2015)].

[59] B. Aubert, M. Bona, D. Boutigny, Y. Karyotakis, J. Lees, V. Poireau, X. Prudent, V. Tisserand, A. Zghiche, J. G. Tico, *et al.*, *Physical Review D* **77**, 092002 (2008).

[60] J. P. Lees, V. Poireau, and e. a. Tisserand, V (BaBar Collaboration), *Phys. Rev. D* **101**, 012011 (2020).

[61] B. Aubert, R. Barate, D. Boutigny, F. Couderc, Y. Karyotakis, J. Lees, V. Poireau, V. Tisserand, A. Zghiche, E. Grauges, *et al.*, *Physical Review D* **73**, 052003 (2006).

[62] B. Aubert *et al.* (BaBar), *Phys. Rev. D76*, 092005 (2007), [Erratum: *Phys. Rev.D77*,119902(2008)], arXiv:0708.2461 [hep-ex].

[63] M. Coupland, E. Eisenhandler, W. R. Gibson, P. Kalmus, and A. Astbury, (1977).

[64] M. Tanabashi *et al.* (Particle Data Group), *Phys. Rev. D98*, 030001 (2018).

[65] T. Barnes, F. Close, P. Page, and E. Swanson, *Phys.Rev. D55*, 4157 (1997), arXiv:hep-ph/9609339 [hep-ph].

[66] J. H. Valencia, *J. Phys. G* **33** (2006).

[67] T. Collaboration and A. Al., *European Physical Journal C* **21**, 261 (2001).

[68] K. Kittimanapun, K. Khosonthongkee, C. Kobdaj, P. Suebka, and Y. Yan, *Phys.rev.c* **79**, 025201 (2009).

[69] V. E. Barnes, S. U. Chung, R. L. Eisner, E. Flaminio, P. Guidoni, J. B. Kinson, and N. P. Samios, *Physical Review Letters* (1969).

[70] D. V. Amelin, E. B. Berdnikov, S. I. Bityukov, G. V. Borisov, V. A. Dorofeev, R. I. Dzhelyadin, Y. P. Gouz, I. A. Kachaev, K. Y. A. Khokhlov, and E. Al., *Zeitschrift für Physik C Particles&Fields* (1996).

[71] N. Armenise, A. Forino, and A. Cartacci, *Phys.Lett. B26*, 336 (1968).

[72] K. A. Olive *et al.* (Particle Data Group), *Chin. Phys. C38*, 090001 (2014).

[73] A. V. Anisovich, C. A. Baker, C. J. Batty, D. V. Bugg, L. Montanet, V. A. Nikonov, A. V. Sarantsev, V. V. Sarantsev, and B. S. Zou, *Phys. Lett. B* **542**, 19 (2002), arXiv:1109.5817 [hep-ex].

TABLE VII: The total and partial decay widths of the $\omega(4S)$ and $\rho(4S)$, the unit of widths is MeV. The γ value is 6.9-11.3.

$\omega(2330)$		$\omega(2290)$		$X(2240)$	$\rho(2150)$	
Channel	Value	Value	Value	Value	Channel	Value
$\Gamma_{exp.}$	435 \pm 75 [55]	275 \pm 35 [55]	139.8 \pm 23.99 [14]		$\Gamma_{exp.}$	310 \pm 140 [62]
Total	372 \pm 170	346 \pm 158	306 \pm 140		Total	310
$\rho(1450)\pi$	134	122	95.8		$\pi\omega_3$	58.6
$\rho\pi$	62.6	68.0	69.0		$a_2\pi(1700)$	40.7
$b_1\pi$	61.6	54.4	42.4		$\pi\pi(1300)$	32.1
$a_1\rho$	37.2	39.0	37.3		$\pi\omega$	31.5
$\rho_3\pi$	19.5	17.3	12.9		$a_2\pi$	23.1
KK_1	8.39	8.33	6.69		$h_1\pi$	14.7
$f_1\omega$	7.84	6.28	4.28		$a_1\pi$	13.6
ηh_1	7.01	7.53	7.54		$b_1\rho$	11.5
K^*K^*	5.91	5.65	4.88		$\pi\pi$	11.4
$\eta\omega$	4.81	3.28	1.70		$a_1\omega$	10.5
$KK(1460)$	4.81	3.45	2.00		$\omega\pi$	8.31
$a_2\rho$	2.65	11.5	19.0		$\rho\rho$	7.74
KK	0.599	0.503	0.379		K'_1K	6.47
KK'_1	0.421	0.224	0.0783		$f_2\rho$	6.19
K^*K_1	0.164	0.152	0.0761		$\pi_2\pi$	5.98
$KK^*(1430)$	0.121	0.0366	0.00138		ωa_0	5.49
$f_2\omega$	0.0228	1.39	4.97		$a_2\omega$	5.34
					$f_1\rho$	4.99
					K^*K^*	4.20
					$K^*(1410)K$	2.92
					$b_1\eta$	1.74
					$KK(1460)$	1.20
					$\rho\eta$	0.99
					$\eta\rho(1450)$	0.903

TABLE VIII: The partial decay widths of the $\omega(1D)$, $\rho(1D)$, the unit of widths is MeV. The γ value is 4.14-6.3.

$\omega(1650)$, $\Gamma_{exp.} = 315 \pm 35$ [64]			$\rho(1700)$, $\Gamma_{exp.} = 250 \pm 100$ [64]		
Channel	Value	Ref. [65]	Channel	Value	[65]
Total	284 ± 113	542	Total	250	435
$b_1\pi$	272	371	$a_1\pi$	93.9	134
$\rho\pi$	42.1	101	$h_1\pi$	85.2	124
KK	9.00	35	$\rho\rho$	26.4	14
$\eta\omega$	7.84		$\omega\pi$	14.1	35
KK^*	5.29	21	KK	9.84	36
			$\eta\rho$	8.76	
			KK^*	6.69	
			$a_2\pi$	2.64	

TABLE XI: The partial decay widths of the $\omega_3(1D)$, $\rho_3(1D)$, the unit of widths is MeV. The γ value is 7.5-9.2.

$\omega_3(1670)$, $\Gamma_{exp.} = 90 \pm 20$ [69]		$\rho_3(1690)$, $\Gamma_{exp.} = 190 \pm 40$ [55]	
Channel	Value	Channel	Value
Total	81.8 ± 16.5	Total	190
$\pi\rho$	62.8	$\rho\rho$	105
$b_1\pi$	14.7	$\pi\pi$	32.0
$\eta\omega$	2.76	$\pi\omega$	23.1
KK	1.16	πh_1	10.6
		πa_2	8.07
		$\eta\rho$	3.68
		πa_1	3.26
		KK	2.66

TABLE X: The partial decay widths of the $\omega(3D)$, $\rho(3D)$, Exp Γ means the experimental total width, the unit of widths is MeV. The γ value is 11.3-14.6.

$\omega(2205)$		$X(2220)$	$\rho(2270)$	
Channel	Value	Value	Channel	Value
$\Gamma_{exp.}$	350 ± 90 [55]	59 ± 30.6 [1]	$\Gamma_{exp.}$	325 ± 80 [10]
Total	147 ± 36.1	164 ± 40.4	Total	325
$b_1\pi$	56.7	66.0	ωa_2	67.0
$\pi\rho(1450)$	21.0	23.7	$\pi\pi(1300)$	64.3
ρa_1	23.7	22.0	πh_1	42.2
ρa_2	9.08	12.2	$\pi\pi$	39.4
$\rho\pi$	8.32	9.78	πa_1	26.1
$\pi\rho_3$	6.09	6.97	$\pi\pi_2$	23.2
ωf_2	5.20	6.59	$\rho\rho$	19.5
ωf_1	5.24	5.54	ρf_2	12.0
KK_1	4.78	4.58	$a_1\omega$	5.81
$\pi\rho(1700)$	2.65	2.90	ρf_1	5.67
ηh_1	2.49	3.41	$\omega\pi$	4.51
$\rho\pi(1300)$	1.34	0.495	KK_1	4.00
			$\rho\rho(1450)$	4.00
			$\pi\omega_3$	3.41
			ηb_1	2.58
			$\omega(1650)\pi$	1.5

TABLE XII: The partial decay widths of the $\omega_3(2D)$, $\rho_3(2D)$, the unit of widths is MeV. The γ value is 10.4-11.8.

$\omega_3(1945)$, $\Gamma_{exp.} = 115 \pm 22$ [55]		$\rho_3(1990)$, $\Gamma_{exp.} = 188 \pm 24$ [10]	
Channel	Value	Channel	Value
Total	105 ± 13.2	Total	188
$b_1\pi$	38.5	$\pi\pi(1300)$	40.6
$\pi\rho$	22.1	πa_2	34.2
$\pi\rho(1450)$	18.7	$\rho\rho$	26.9
$\rho_3\pi$	11.5	πa_1	16.7
$\eta\omega$	4.51	πh_1	16.4
$h_1\eta$	4.44	$\pi\omega(1420)$	15.5
K^*K^*	2.31	$\pi\pi_2$	9.19
KK^*	1.28	$\pi\omega_3$	7.80
		$\pi\omega$	7.14
		$\eta\rho$	4.58
		ηb_1	2.63
		K^*K^*	2.54
		KK^*	1.61

TABLE XIII: The partial decay widths of the $\omega_3(3D)$, $\rho_3(3D)$, the unit of widths is MeV. The γ value is 6.7-12.5.

$\omega_3(2285)$, $\Gamma_{exp.} = 224 \pm 50$ [11]		$\rho_3(2250)$, $\Gamma_{exp.} = 135 \pm 75$ [63]	
Channel	Value	Channel	Value
Total	226 ± 126	Total	135
$a_2\rho$	76.3	ωa_2	58.5
$\pi\rho$	32.6	ρf_2	33.7
$f_2\omega$	25.6	$\pi\omega$	12.3
$b_1\pi$	24.5	$\rho\rho$	11.6
$\rho_3\pi$	12.9	πh_1	11.0
$\pi(1300)\rho$	10.8	πa_2	9.26
$\pi\rho(1450)$	5.22	πa_1	8.60
$a_1\rho$	4.37	$\pi\omega_3$	4.32
$\eta\omega$	3.78	$\pi\pi$	3.68
$\eta\omega(1420)$	3.68	$\pi\pi_2$	2.95
$h_1\eta$	3.28	$\pi\omega(1420)$	2.70
$\eta(1295)\omega$	2.14	ηb_1	2.09
K^*K^*	1.45	$KK^*(1410)$	2.06
		ωa_1	1.92
		$\eta\rho$	1.82
		$\rho\eta(1295)$	1.81
		$\eta\rho(1450)$	1.70
		K^*K^*	1.69

TABLE XIV: The partial decay widths of the $\omega_3(4D)$, $\rho_3(4D)$, the unit of widths is MeV. The γ value is 11.6.

$\omega_3(2630)$		$\rho_3(2630)$	
Channel	Value	Channel	Value
Total	288	Total	420
$a_2\rho$	57.2	$a_4(2040)\pi$	184
$\pi(1300)\rho$	40.3	$a_2(1700)\omega$	38.7
$b_1\pi$	37.3	$a_2(1700)\pi$	35.4
$\pi\rho$	33.3	$a_2\pi$	25.3
$\pi\rho(1450)$	32.8	$\rho\rho(1450)$	22.4
$\rho_3\pi$	23.0	$f_2\rho$	16.9
$f_2\omega$	17.2	$h_1\pi$	14.3
$\eta(1295)\omega$	8.03	$b_1\rho$	11.8
$\pi_2\rho$	6.85	$\omega(1420)\pi$	10.2
$\eta\omega(1420)$	6.42	$\omega_3\pi$	8.75
$K^*K^*(1410)$	5.65	$\rho\rho$	6.76
$h_1\eta$	5.30	$\pi_2\pi$	6.65
$\eta\omega$	3.46	$K^*K^*(1410)$	5.65
$K^*K_2^*$	2.36	$\rho(1450)\eta$	5.51
f_2h_1	1.94	$\pi\pi$	4.79
$\eta_2\omega$	1.86	$b_1\eta$	4.01
$f_1\omega$	1.66	$a_1\omega$	3.27
a_2b_1	1.50	$K_2^*K^*$	2.36
f_1h_1	1.09	$\pi_2\omega$	2.14
$\pi\rho(1700)$	1.01	h_1a_1	1.94
		b_1b_1	1.83
		$K^*(1410)K$	1.71
		a_2h_1	1.51
		$\rho(1450)\eta'$	1.39
		$\pi\pi(1300)$	1.21
		$h_1\pi(1300)$	1.04

TABLE XV: The partial decay widths of the $\omega_3(1G)$, $\rho_3(1G)$, the unit of widths is MeV. The γ value is 11.6.

$\omega_3(2255)$, $\Gamma_{exp.} = 175 \pm 30$ [55]		$\rho_3(2255)$	
Channel	Value	Channel	Value
Total	325	Total	721
$b_1\pi$	147	$\pi_2\pi$	296
$\rho_3\pi$	47.0	$b_1\rho$	76.5
$h_1\eta$	32.9	$\rho\rho$	62.6
$a_2\rho$	23.2	$a_1\pi$	57.4
$\pi\rho$	17.4	$h_1\pi$	46.2
KK'_1	12.5	$a_2\pi$	37.1
$f_2\omega$	11.3	$b_1\eta$	31.5
$\pi\rho(1450)$	8.69	$a_1\omega$	28.9
$\pi(1300)\rho$	5.32	$\omega_3\pi$	16.6
$\eta\omega$	4.00	$\pi\pi(1300)$	14.2
$\pi\rho(1700)$	2.57	$f_2\rho$	12.2
KK_1	2.53	K'_1K	11.7
KK'_2	2.20	$\omega\pi$	5.86
$\eta'\omega$	1.75	$a_2(1700)\pi$	5.02
$a_1\rho$	1.75	$\omega(1420)\pi$	3.01
$\omega_3\eta$	1.52	$\pi\pi$	2.90
$\eta\omega(1420)$	1.05	K_1K	2.82
$\eta(1295)\omega$	1.04	K'_2K	2.20
KK^*	1.03	$f_1\rho$	2.201
		$\rho\eta'$	1.87
		$\omega(1650)\pi$	1.54
		$b_1\eta'$	1.27
		$\rho\eta(1295)$	1.15
		K^*K	1.03

TABLE XVI: The partial decay widths of the $\omega_3(2G)$, $\rho_3(2G)$, the unit of widths is MeV. The γ value is 11.6.

$\omega_3(2520)$		$\rho_3(2520)$	
Channel	Value	Channel	Value
Total	312	Total	397
$b_1\pi$	107	$\pi_2\pi$	107
$a_2\rho$	40.9	$h_1\pi$	37.1
$\pi_2\rho$	21.4	$a_1\pi$	36.0
$\rho_3\pi$	19.4	$\rho\rho(1450)$	31.4
$h_1\eta$	18.9	$a_1\omega$	22.6
$\pi\rho$	18.6	$b_1\rho$	21.0
$f_2\omega$	17.5	$f_2\rho$	18.4
KK_2	15.3	$b_1\eta$	16.4
$f_1\omega$	13.2	$a_2(1700)\pi$	16.4
$a_0\rho$	9.88	$a_2\pi$	16.04
$\pi(1300)\rho$	4.88	$\rho\rho$	9.21
$\eta_2\omega$	3.57	$\pi_2\omega$	7.03
f_1h_1	3.03	$\omega_3\pi$	6.81
$h_1\eta(1295)$	3.16	b_1b_1	6.46
f_2h_1	3.11	$a_4(2040)\pi$	6.16
$\eta\omega$	3.08	$\pi\pi$	6.15
$f_1(1420)\omega$	3.03	$f_1\rho$	4.72
$h_1\eta'$	2.63	$h_1\pi(1300)$	4.35
$\omega_3\eta$	1.81	K'_2K	3.81
$a_1\rho$	1.31	$a_2\omega$	3.50
$\eta'\omega$	1.06	$f_1(1420)\rho$	3.20
		ωa_0	3.08
		h_1a_1	2.52
		a_2h_1	2.18
		$\rho_3\eta$	1.50
		$KK(1630)$	1.42
		$\pi\pi(1300)$	1.38
		$b_1\eta'$	1.31

TABLE XVII: The partial decay widths of the $\omega_3(3G)$, $\rho_3(3G)$, the unit of widths is MeV. The γ value is 11.6.

$\omega_3(2750)$		$\rho_3(2750)$	
Channel	Value	Channel	Value
Total	181	Total	270
$b_1\pi$	63.8	$\pi_2\pi$	46.0
$\pi\rho$	12.3	$\rho\rho$	24.3
$\rho_3\pi$	12.0	$h_1\pi$	24.0
$f_1\omega$	11.7	$a_1\omega$	23.6
$\pi_2\rho$	10.4	$a_1\pi$	21.0
$h_1\eta$	9.84	$a_2\pi$	10.5
$b_1\pi(1300)$	8.28	$a_2(1700)\pi$	9.40
$f_2\omega$	8.25	$f_2\rho$	8.45
$\pi(1300)\rho$	7.77	$\rho\eta(1295)$	8.17
$a_2\rho$	5.59	$\rho\rho(1450)$	7.91
$\pi\rho(1450)$	5.32	$b_1\eta$	7.90
$a_0\rho$	4.89	$b_1\rho$	7.84
$h_1\eta(1295)$	4.21	$a_2(1700)\omega$	7.05
$\eta_2\omega$	1.96	$h_1\pi(1300)$	6.56
$f_1(1420)\omega$	1.85	$\pi\pi$	6.40
$\eta\omega$	1.59	$\omega_3\pi$	4.30
f_2h_1	1.59	$\omega\pi$	4.040
$\eta(1295)\omega$	1.55	$a_4(2040)\pi$	3.94
K_1K_1	1.50	$\pi_2\omega$	3.55
$\eta\omega(1420)$	1.50	$\omega\pi(1300)$	2.62
$a_1\rho$	1.37	$a_1\pi(1300)$	2.17
KK'_1	1.34	$f_1(1420)\rho$	1.96
$\omega_3\eta$	1.07	$a_1\omega(1420)$	1.86
$h_1\eta'$	1.01	$b_1\eta(1295)$	1.84
		$a_2\omega$	1.69
		$\rho\eta(1475)$	1.64
		$a_2(1320)h_1$	1.55
		b_1b_1	1.54
		b_1f_1	1.51
		K_1K_1	1.50
		$\rho(1450)\eta$	1.48
		ωa_0	1.48
		$\omega(1420)\pi$	1.43
		h_1a_1	1.39
		$\pi(1300)\pi(1300)$	1.19
		a_2a_2	1.03